Available online at www.sciencedirect.com
ScienceDirect
Journal of Sound and Vibration 305 (2007) 827–842
JOURNAL OF SOUND AND VIBRATION
www.elsevier.com/locate/jsvi

Symmetric wave corrections to the line driven, fluid loaded, thin elastic plate

John D. Smith*

Defence Science and Technology Laboratory, Porton Down, Salisbury, Wilts SP4 0JQ, UK

Received 10 March 2006; received in revised form 8 March 2007; accepted 1 May 2007
Available online 18 June 2007

Abstract

The effect of coupling between in-plane (symmetric wave) plate vibrations and the acoustic field are investigated in the context of thin plate theory. Comparisons are made of the reflection and transmission coefficients with the results of three-dimensional elasticity and the fluid loaded dispersion curves are considered. The response of a line driven, fluid loaded, air-backed thin plate is calculated and it is shown that symmetric wave corrections can give contributions at leading order, for certain ranges of angle or frequency.

1. Introduction

The acoustic radiation and structural response of a driven elastic plate immersed in a fluid is a cornerstone of structural acoustics. Although modern structural acoustics makes extensive use of finite element (FE) codes and numerical techniques, most of the fundamental understanding of this problem is based on the use of shell theory [1,2]. The foundations of this understanding were laid in the 1960s with the work of Feit [3], and Maidanik and Kerwin [4]. Significant progress was then achieved by Crighton who, in a series of papers through the 1980s, advocated an approach based on perturbation expansions in a fluid loading parameter, ε [5–7]. This work is summarised in his Rayleigh medal lecture [8]. Recent work has focused on extending the frequency range of these results [9] and looking at the effects of attached inhomogeneities [10].

Most work to date has focused on shell theories that are transversely inextendable, i.e., they are based on the Kirchoff–Love approximation that "normals to the undeformed middle surface remain straight and normal to the deformed middle surface and *suffer no extension*" [11]. This has the consequence that the structural response to a driving force normal to the plate is determined solely by the bending wave equation and there is no coupling to in-plane vibrations. In this paper the effects of using a shell theory that allows transverse extendability are considered. It is shown that in this case in-plane (symmetric wave) vibrations are excited in the plate, both by the driving force and by coupling from the acoustic field. In most cases the effect of these vibrations on the acoustic radiation and structural response is small and can be safely ignored

*Tel.: +44 1980 614897; fax: +44 1980 613521.
E-mail address: jdsmith@dstl.gov.uk

0022-460X/$ - see front matter
doi:10.1016/j.jsv.2007.05.006

however, in certain ranges of angle or frequency, these effects occur at leading order and should be retained in addition to the usual bending wave contributions.

Some effects of symmetric waves on the radiation of plates have been considered before: Rudgers et al. [12] used a modified thick plate theory to calculate the radiation from a variety of metallic and polymeric plates. The computations are based on the analysis of Feit [3] and radiation at the coincidence angle for symmetric waves is demonstrated. The approach used here is similar to Crighton's [8], and the aim is to understand how the symmetric wave corrections lead to significant effects at all frequencies despite, on the face of it, appearing to be higher order corrections. By deriving the thin plate equations in a consistent way it can be seen that any shell theory that uses the Kirchoff–Love approximation as its basis will contain no coupling between the acoustic field and the symmetric plate waves when the shell approximates a flat plate. This has implications for the types of shell theory that should be used for deriving shell elements in FE analyses of structural acoustic problems.

The paper is divided as follows: Section 2 derives the plate equations for a forced, fluid loaded thin flat plate from a variational principle. Section 3 then uses these plate equations to derive expressions for the reflection and transmission coefficients of an elastic plate fully immersed in a fluid. Here exact results from the full elastic theory are easy to obtain and the results of the thin shell theory are compared with both the full theory and the result of keeping only the bending wave contribution. Section 4 looks at asymptotic results for the dispersion curves of both a fully immersed plate and of an air-backed, fluid loaded, plate. Section 5 then looks at the case of a line driven, air-backed, fluid loaded plate (the case usually of most interest) and calculates the acoustic radiation and structural response.

2. The plate equations

First the plate equations for a forced, fluid loaded, flat plate are derived. The approach is based on the variational principle of Kohn et al. [13]. This is related to Hamilton's principle though any variational method that satisfied the correct stress boundary condition on the surface of the plate would, in principle, give the same result [14]. For an elastic solid with Lamé constants λ, μ and density ρ, taking up volume V with surface ∂V, the steady-state action functional is given by

$$J = \int_V \{\rho\omega^2 U_\alpha U_\alpha^* - \lambda\,\varepsilon_{\alpha\alpha}\varepsilon_{\beta\beta}^* - 2\mu\,\varepsilon_{\alpha\beta}\varepsilon_{\beta\alpha}^*\}\,\mathrm{d}V + \int_{\partial V} f_\alpha U_\alpha^*\,\mathrm{d}S. \tag{1}$$

The U_α are the components of the elastic displacements of the material in a Cartesian coordinate system, with Greek indices running over the set (x, y, z). Summation over repeated indices is assumed and '$*$' denotes complex conjugate. Surface tractions are given by the vector field, f_α, and the integrals are over the volume and surface area, respectively. Harmonic time dependence, $\mathrm{e}^{-\mathrm{i}\omega t}$, is assumed throughout the paper.

Taking the strain tensor to have its small displacement form

$$\varepsilon_{\alpha\beta} = \tfrac{1}{2}(\partial_\alpha U_\beta + \partial_\beta U_\alpha) \tag{2}$$

(∂_α standing for the partial derivative with respect to the α coordinate), the relationship between the stress tensor, $\sigma_{\alpha\beta}$, and the strain is given by

$$\sigma_{\alpha\beta} = \lambda\,\varepsilon_{\gamma\gamma}\delta_{\alpha\beta} + 2\mu\varepsilon_{\alpha\beta}, \tag{3}$$

where $\delta_{\alpha\beta}$ is the Kronecker delta. It is then a straightforward matter to show that minimising J with respect to variations in the complex conjugate displacement, U_α^*, leads to the usual three-dimensional steady-state elastic equations of motion

$$\partial_\beta\sigma_{\alpha\beta} + \rho\omega^2 U_\alpha = 0 \tag{4}$$

together with the boundary condition

$$f_\alpha = \sigma_{\alpha\beta} n_\beta \tag{5}$$

on ∂V, which has outward unit normal n_α [13]. The Lamé constants can be related to the Young's modulus, E and Poisson's ratio ν by the relations

$$\lambda = \frac{E\nu}{(1-2\nu)(1+\nu)} \quad \text{and} \quad \mu = \frac{E}{2(1+\nu)}. \tag{6}$$

If the volume V consists of two materials—one occupying volume V_0 and the other V_1—with common boundary $S_c = \partial V_0 \cup \partial V_1$, then the volume integral in Eq. (1) is split into separate volume integrals for V_0 and V_1. Minimising J with respect to the complex displacements leads to integrals of the form

$$\int_{V_{0,1}} \{\rho\omega^2 U_\alpha + \partial_\beta \sigma_{\alpha\beta}\} \delta U^*_\alpha \, \mathrm{d}V \tag{7}$$

together with a surface integral over the interface between the two materials

$$\int_{S_c} (\sigma_{0\alpha\beta} \delta U^*_{0\beta} - \sigma_{1\alpha\beta} \delta U^*_{1\beta}) n_{0\alpha} \, \mathrm{d}S, \tag{8}$$

where $\sigma_{0\alpha\beta}$, $U_{0\beta}$ are the assumed forms for the stress tensor and displacement vector in material 0 and similarly for material 1. Use has been made of the fact that $n_{0\alpha} = -n_{1\alpha}$ on the common boundary.

The volume integral contributions to δJ imply that the equations of motion (4) hold separately in each material. The surface integral (8) then leads to interface conditions that must hold between the materials. Physically it would be expected that the displacement should be continuous across the interface and hence the variation should be restricted to trial functions that satisfy this condition. This could be enforced formally by the addition of a Lagrange multiplier term to Eq. (1) if desired [15]. For continuous displacements, Eq. (8) then implies that the components of the stress tensor in the direction of the surface normal must be continuous, i.e.,

$$\sigma_{0\alpha\beta} n_{0\beta} = \sigma_{1\alpha\beta} n_{0\beta}. \tag{9}$$

In the case when V_0 contains a fluid, the shear modulus, μ, in V_0 is taken to be zero and thus $\lambda = K$, which is the bulk modulus of the fluid. Since the only contribution to the stress tensor in the fluid is through the divergence of $\mathbf{U}$, Eq. (4) can be used to show that $\mathbf{U}$ must have zero curl. The equation of motion in the fluid (4) then simply becomes

$$\nabla^2 U_\alpha + \left(\frac{\omega}{c_0}\right)^2 U_\alpha = 0, \tag{10}$$

with $c_0 = \sqrt{K/\rho_0}$ and the stress tensor is given by

$$\sigma_{\alpha\beta} = K(\nabla_\gamma U_\gamma)\delta_{\alpha\beta} = -p\,\delta_{\alpha\beta}, \tag{11}$$

where p is the acoustic pressure [16]. Since Eq. (8) now only contains the components of displacement normal to the interface, only these components need to be continuous.

It can be seen that Eqs. (10) and (9) are the usual steady-state equations of motion and interface conditions for an acoustic fluid, which are usually derived directly from Euler's equation and the equation of continuity for the fluid [17]. Eq. (10) can be recast in terms of the pressure simply by taking the divergence of each side. Hence, without any loss of generality, the variational principle (1) will be used only to obtain effective equations for the elastic plate and any surrounding fluid will be taken to satisfy the usual Helmholtz equation of motion and interface conditions with its only contribution to Eq. (1) being through the forces it exerts on the surface of the plate.

To proceed, the plate is assumed to lie in the x–y plane, with mid-plane at $z = 0$ and to have thickness $2h$. Traditional plate theory assumes that the thickness of the plate is small compared to the lateral dimensions of the plate and the longitudinal and shear wavelengths, allowing the displacements to be expanded as a power series in z [11]. Taking the Latin indices, $i,j,k,\ldots$, to stand for the in-plane components (x,y), this motivates the following ansatz for the plate displacements:

$$U_i(x,y,z) = u_i(x,y) + z v_i(x,y) + \tfrac{1}{2} z^2 t_i(x,y), \tag{12a}$$

$$U_z(x,y,z) = w_0(x,y) + zw_1(x,y) + \tfrac{1}{2}z^2 w_2(x,y). \tag{12b}$$

The Kirchoff–Love approximation corresponds to taking w_1 and w_2 identically equal to zero [18].

The elastic strains can then be calculated to first order in z as

$$\varepsilon_{ij} = \tfrac{1}{2}(\partial_i u_j + \partial_j u_i) + \tfrac{1}{2}z(\partial_i v_j + \partial_j v_i), \tag{13a}$$

$$\varepsilon_{iz} = \varepsilon_{zi} = \tfrac{1}{2}(\partial_i w_0 + v_i) + \tfrac{1}{2}z(\partial_i w_1 + t_i), \tag{13b}$$

$$\varepsilon_{zz} = w_1 + zw_2. \tag{13c}$$

If it is assumed there is a fluid, with pressure p, filling the half-space $z>h$ and the lower side of the plate is driven using a normal driving force, $f(x,y)$, then the boundary conditions on the stress in the plate are

$$\sigma_{zz} = -p, \quad \sigma_{iz} = 0 \quad \text{at } z = h \tag{14a}$$

and

$$-\sigma_{zz} = f, \quad \sigma_{iz} = 0 \quad \text{at } z = -h. \tag{14b}$$

Using the first-order form of the strain (13) to calculate the stress then gives

$$v_i = -\partial_i w_0, \tag{15a}$$

$$t_i = -\partial_i w_1, \tag{15b}$$

$$w_1 = -\frac{(f+p)}{2(\lambda+2\mu)} - \gamma\partial_i u_i \tag{15c}$$

and

$$w_2 = \frac{(f-p)}{2h(\lambda+2\mu)} + \gamma\partial_i\partial_i w_0, \tag{15d}$$

where $\gamma = \lambda/(\lambda+2\mu) = \nu/(1-\nu)$. The only unknowns are thus the displacements of the mid-plane of the plate.

Substituting these results into the functional (1) and performing the integration over z leads to

$$\begin{aligned} J = \frac{2hE}{1-\nu^2}\int \mathrm{d}S\{&-\nu\partial_i u_i\partial_j u_j^* - (1-\nu)(\partial_i u_j + \partial_j u_i)\partial_i u_j^* \\ &- \nu I\partial_i\partial_i w_0\partial_j\partial_j w_0^* - (1-\nu)I\partial_i\partial_j w_0\partial_i\partial_j w_0^* + \Omega(u_i u_i^* + w_0 w_0^*)\} \\ &+ \int \mathrm{d}S[(f-p)w_0^* + (f+p)h\gamma\partial_i u_i^*]. \end{aligned} \tag{16}$$

The surface integral is to be taken over the area of the plate, $I = h^2/3$ is the square of the radius of gyration of the plate and $\Omega = \rho\omega^2(1-\nu^2)/E$. Rotary inertia terms of the form $\rho h^2/3$ have been neglected.

It is now a straightforward matter to perform the variations over u_i^* and w_0^*. Setting the resulting integrals to zero implies the plate equations

$$\frac{(1+\nu)}{2}\partial_i\partial_j u_j + \frac{(1-\nu)}{2}\partial_j\partial_j u_i + k_p^2 u_i = \frac{\gamma}{2\rho c_p^2}\partial_i(f+p), \tag{17a}$$

$$\partial_i\partial_i\partial_j\partial_j w_0 - k_b^4 w_0 = \frac{1}{2h\rho c_b^2}(f-p), \tag{17b}$$

where $c_p^2 = E/\rho(1-\nu^2)$ and $c_b^2 = IE/\rho(1-\nu^2)$. One thus sees that the thin plate equations are a natural consequence of the stress satisfying the correct boundary conditions on the surfaces of the plate to first order in h. It should be noted that the derivative term on the right-hand side of Eq. (17a) came from the U_z^* term in the surface integral of Eq. (1) and would not be present if w_1 had been taken to be zero.

Taking the normal displacement to first order then gives

$$U_z = w_0 - z\left(\frac{f+p}{2\rho c_l^2} + \gamma \partial_i u_i\right), \tag{18}$$

where use has been made of the longitudinal wave speed, $c_l = \sqrt{(\lambda + 2\mu)/\rho}$. This procedure can be extended to finite plates and curved shells.

3. The reflection and transmission coefficients

The problem of a plane wave incident on an infinite elastic plate fully immersed in a fluid is now considered. The plate lies in the x–y plane and has its mid-plane at $z = 0$. Surrounding the plate is a compressible fluid with density ρ_0 and sound speed c_0, which satisfies the Hemholtz equation

$$\nabla^2 p_\pm + k_0^2 p_\pm = 0 \tag{19}$$

for the acoustic pressure, $p_+(\mathbf{x})$ for $z > h$ and $p_-(\mathbf{x})$ for $z < -h$. A plane wave of wavenumber $k_0 = \omega/c_0$ is incident in the z–x plane, from $z = \infty$ and at an angle θ to the normal of the plate. These conditions are such that the acoustic field and plate displacements can be considered to be independent of y and the problem is two-dimensional. The geometry is as shown in Fig. 1.

In Section 2 it was shown that the linear response of a thin plate subjected to a normal driving force $f(x)$ on the face at $z = -h$, and with a pressure $p(x)$ over the face at $z = h$ is determined by the plate equations

$$\frac{\mathrm{d}^2 2u_x}{\mathrm{d}x^2} + k_p^2 u_x = \frac{\gamma}{2\rho c_p^2}\frac{\mathrm{d}}{\mathrm{d}x}(f+p), \tag{20}$$

$$\frac{\mathrm{d}^4 w_0}{\mathrm{d}x^4} - k_b^4 w_0 = \frac{1}{2h\rho c_b^2}(f-p). \tag{21}$$

Eq. (20) governs the x-component (in-plane) of the displacement vector of the mid-plane of the plate; it gives a low-frequency approximation to the lowest order symmetric wave which, in vacuum, has wavenumber $k_p = \omega/c_p$ and phase velocity c_p. This equation differs from the one obtained using the Kirchoff–Love inextendable assumption [11] by the presence of the forcing term on the right-hand side, which is proportional to $\gamma = \nu/(1-\nu)$. This force has a simple physical interpretation: a pressure gradient causes an in-plane displacement in the plate through the Poisson's ratio of the material. Thus it is absent if the plate

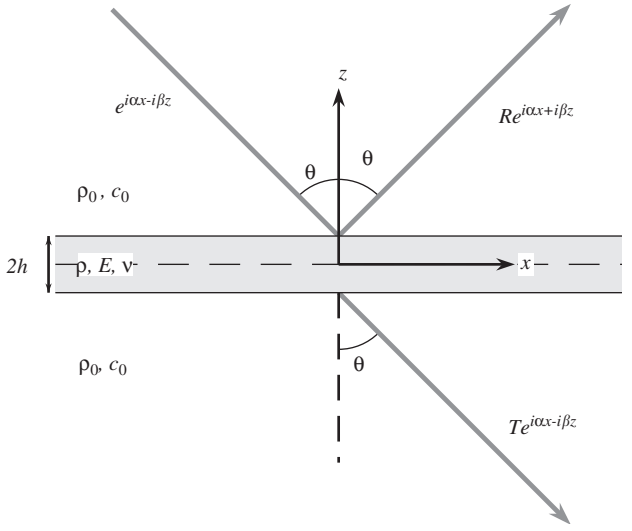

Fig. 1. Geometry of the fluid-plate system showing incoming plane wave, reflected wave and transmitted wave. In Section 5 the lower fluid half-space is replaced with a normal driving force, $f(x)$.

displacements are restricted to a form that allows no local change in the thickness of the plate, as measured along the normals to the mid-plane. Eq. (21) is the usual bending wave equation, with vacuum wavenumber $k_b = \sqrt{\omega/c_b}$. If the thickness of the plate is taken to be $H = 2h$, then c_b is given by $c_b = \sqrt{B/m}$, where $B = \sqrt{EH^3/12(1-\nu^2)}$ is the bending stiffness of the plate and $m = H\rho$ is the mass per unit area. It should be noted that c_b is not the phase velocity of the plate: that is given by $\sqrt{\omega c_b}$.

In addition to the equations of motion, the correct boundary conditions must be satisfied on the faces of the plate. The system of Eqs. (20) and (21) was derived by ensuring the displacements in the plate are such that the stress boundary conditions on the surfaces of the plate are satisfied to order h. For consistency, the normal displacement in the fluid at the surface of the plate should match that of the plate to the same order. In the plate, it is given by

$$U_z \simeq w_0(x) - z\left(\frac{f+p}{2\rho c_l^2} + \gamma\frac{\mathrm{d}u_x}{\mathrm{d}x}\right). \tag{22}$$

When $z = \pm h$ this should be equal to the z-component of the displacement in the fluid which, for harmonic time dependence $\mathrm{e}^{-\mathrm{i}\omega t}$, is given by

$$U_z = \frac{1}{\rho_0\omega^2}\frac{\partial p_\pm}{\partial z}. \tag{23}$$

To find the reflection and transmission coefficients of the plate, $p = p_+(x,h)$ and f is taken to be the force exerted on the plate by the transmitted pressure wave, i.e., $f = p_-(x,-h)$. Taking

$$p_+ = \mathrm{e}^{\mathrm{i}\alpha x - \mathrm{i}\beta(z-h)} + R\mathrm{e}^{\mathrm{i}\alpha x + \mathrm{i}\beta(z-h)}, \quad p_- = T\mathrm{e}^{\mathrm{i}\alpha x - \mathrm{i}\beta(z+h)}, \tag{24}$$

with $\alpha = k_0\sin\theta$ and $\beta = k_0\cos\theta$, a periodic ansatz can be chosen for $u_x(x)$ and $w_0(x)$ viz.,

$$u_x = U\mathrm{e}^{\mathrm{i}\alpha x} \quad \text{and} \quad w_0(x) = W\mathrm{e}^{\mathrm{i}\alpha x}. \tag{25}$$

Substituting this ansatz into Eqs. (20) and (21) allows the amplitudes U and W to be expressed in terms of R and T. Setting Eq. (22) equal to Eq. (23) when $z = \pm h$ then leads to a pair of simultaneous equations for the reflection and transmission coefficients. These are easily solved to obtain

$$R = \frac{1}{D_A D_B}\left[(k_b^4 - \alpha^4)(k_p^2 - \alpha^2) + \left(\frac{2\mu}{\beta}\right)^2 k_b^4(\gamma^2\alpha^2 k_p^2 h^2 - k_l^2 h^2(k_p^2 - \alpha^2))\right], \tag{26}$$

$$T = \frac{2\mathrm{i}\mu}{\beta D_A D_B}[k_b^4(k_p^2 - \alpha^2) - \gamma^2\alpha^2 k_p^2 h^2(k_b^4 - \alpha^4) + k_l^2 h^2(k_b^4 - \alpha^4)(k_p^2 - \alpha^2)], \tag{27}$$

with

$$D_A = k_b^4 - \alpha^4 + \frac{2\mathrm{i}\mu}{\beta}k_b^4 \tag{28}$$

and

$$D_B = (k_p^2 - \alpha^2)\left(1 - \frac{2\mathrm{i}\mu}{\beta}k_l^2 h^2\right) + \frac{2\mathrm{i}\mu}{\beta}\gamma^2\alpha^2 k_p^2 h^2. \tag{29}$$

The mass ratio, $\mu = \rho_0/2h\rho$.

Fig. 2 shows a comparison of the Insertion Loss (the square of the modulus of the transmission coefficient expressed in dB's) calculated from the expression (27) with that calculated using the full elastic theory [19] for a 10 mm steel plate in water at 35 kHz. There is a discrepancy in the position of the flexural coincidence angle (as is well known [1]—this due to the thin plate theory over predicting the flexural wave speed at these frequencies), however the general features are predicted well. One notes, in particular, the presence of a second coincidence angle associated with the symmetric (in-plane) waves on the plate. This is not predicted by the usual thin plate theory.

The presence of the cusp in the Insertion Loss is due to terms of the form $(k_p h)^2/(\alpha^2 - k_p^2)$ which arise in the continuity condition on the normal displacement; away from the angle defined by

$$\theta_P = \sin^{-1}\left(\frac{c_0}{c_p}\right), \tag{30}$$

the terms of order $(k_l h)^2$ and $(k_p h)^2$, which came from the first-order terms in U_z, are negligible compared to the other terms and Eq. (27) reduces to the usual thin plate theory result

$$T = \frac{2i\mu}{\left(1 - \left(\frac{k_0}{k_b}\right)^4 \sin^4\theta\right) k_0 \cos\theta + 2i\mu}. \tag{31}$$

Near $\theta = \theta_p$ however, the terms of order $(k_p h)^2$ cannot be ignored in comparison to the other terms, leading to the observed cusp.

Fig. 3 shows how this feature changes as the frequency varies. There is no apparent cut-on frequency—as would be the case with the flexural wave [1]—but it becomes broader in angle with increasing frequency and is more obvious above the (flexural) coincidence frequency.

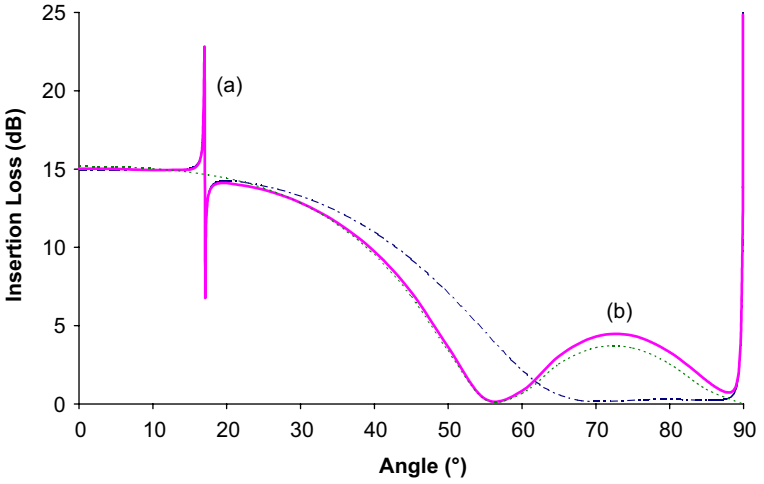

Fig. 2. Comparison of the Insertion Loss (given by $-20\log_{10}|T|$) calculated using the full elastic theory (– · – · –) with that calculated using Eq. (27) (—) and the result of retaining only the bending wave contribution (31) (· · · ·). The position of the coincidence angle for the symmetric wave is marked (a), and that of the flexural wave (b).

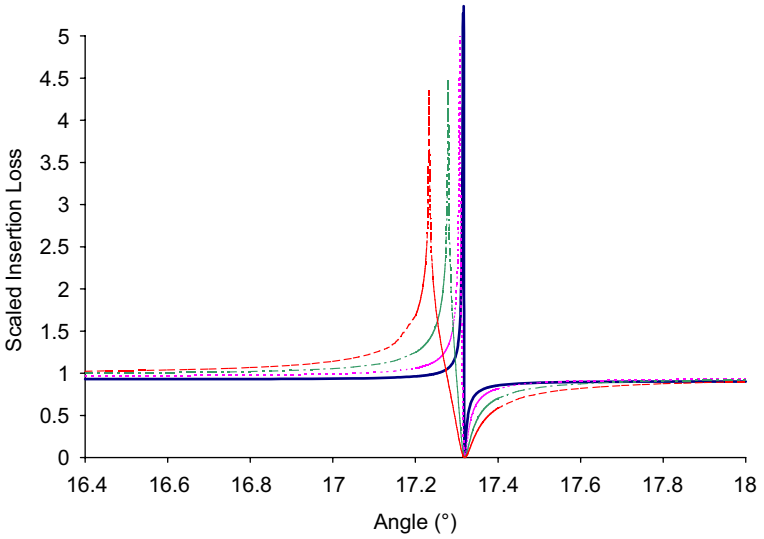

Fig. 3. The change of the cusp in the Insertion Loss versus angle plot with increasing frequency. Each curve is scaled by the Insertion Loss at 0° for comparison purposes. The curves shown are: solid line (—) for 2.4 kHz ($\bar{\omega} = 0.1$), dotted line (· · · ·) for 12.0 kHz ($\bar{\omega} = 0.5$), dots and dashes (– · – · –) for 24.0 kHz ($\bar{\omega} = 1.0$), and dashed line (– – –) for 36.0 kHz ($\bar{\omega} = 1.5$).

It is convenient to define non-dimensional parameters: frequencies are scaled relative to the coincidence frequency, $\omega_c = c_0^2/c_b$, thus $\bar{\omega} = \omega/\omega_c$. The usual fluid loading parameter, ε, is given by

$$\varepsilon = \frac{\rho_0}{2h\rho}\frac{c_b}{c_0}. \tag{32}$$

It has the advantage that it is independent of the plate thickness and is usually small, thus being ideal for perturbation expansions [8]. In addition, two new parameters

$$\alpha_l = \frac{h^2 c_0^4}{c_b^2 c_l^2} \quad \text{and} \quad \alpha_p = \gamma^2 \frac{h^2 c_0^4}{c_b^2 c_p^2} \tag{33}$$

are introduced; again, these parameters depend only on the material properties and are independent of the plate thickness. Since $\gamma^2 k_p^2 h^2 = \alpha_p \bar{\omega}^2$ and $k_l^2 h^2 = \alpha_l \bar{\omega}^2$, they are expected to be small parameters and can usually be dropped except when they occur at leading order in an expansion.

4. The dispersion curves

The dispersion equations for the plate determine the frequency dependence of the wavenumbers of free waves on the plate. They may be obtained by taking travelling wave solutions for u_x and w_0,

$$u_x(x) = U\mathrm{e}^{\mathrm{i}kx}, \quad w_0(x) = W\mathrm{e}^{\mathrm{i}kx} \tag{34}$$

and assuming the acoustic field has the form

$$p_+ = T_u \mathrm{e}^{\mathrm{i}kx + \mathrm{i}\beta(z-h)} \quad \text{for } z > h, \tag{35a}$$

$$p_- = T_b \mathrm{e}^{\mathrm{i}kx - \mathrm{i}\beta(z+h)} \quad \text{for } z < -h, \tag{35b}$$

with $\beta^2 = k_0^2 - k^2$.

For real k, if $k < k_0$ (supersonic wave) the wave in the plate must couple to an outgoing acoustic wave and $\beta = \sqrt{k_0^2 - k^2}$. If $k > k_0$, the acoustic field must decay as $z \to \infty$ and $\beta = \mathrm{i}\sqrt{k^2 - k_0^2}$. When k is complex a branch cut must be chosen, starting from the branch point $k = k_0$, that maintains these conditions on the real k-axis. This has been discussed many times in the literature from the point of view of the forced response (see, for example, Ref. [5]). One can take the view that the solutions to the dispersion problem (35) have no physical meaning except as the kernel of a Fourier transform in solving the forced response, since the solutions with complex k must be divergent at either $x = \pm\infty$. Nevertheless, the dispersion problem with complex k has been studied in it's own right for purposes such as non-destructive evaluation [20]. If one imposes the condition that the solutions for complex k must tend smoothly to the solutions for real k as both the fluid loading and the damping tend continuously to zero, a natural choice for the branch cut is given in Fig. 4.

Using the assumed form of the acoustic field in the continuity condition for the normal displacement at $z = \pm h$, together with the plate equations (20) and (21), leads to a matrix equation for the amplitudes of the free waves on the plate

$$\begin{bmatrix} L_{UU} & L_{UW} \\ L_{WU} & L_{WW} \end{bmatrix} \begin{bmatrix} U \\ W \end{bmatrix} = 0, \tag{36}$$

with

$$L_{UU} = (k^2 - k_p^2)\left(1 - \frac{2\mathrm{i}\mu}{\beta}k_l^2 h^2\right) - \frac{2\mathrm{i}\mu}{\beta}\gamma^2 k_p^2 h^2 k^2, \tag{37a}$$

$$L_{WW} = k^4 - k_b^4 - \frac{2\mathrm{i}\mu}{\beta}k_b^4 \tag{37b}$$

and

$$L_{UW} = L_{WU} = 0. \tag{37c}$$

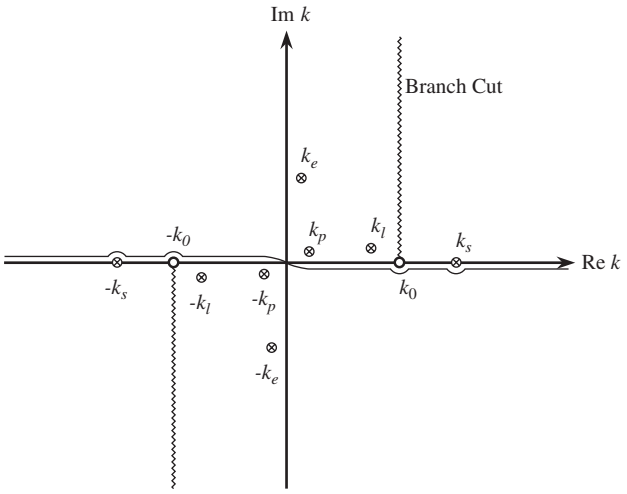

Fig. 4. The complex k plane showing the choice of branch cut and typical positions when $\bar{\omega} > 1$ for the subsonic pole, k_s, the leaky pole, k_l, the evanescent pole k_e and the symmetric wave pole, k_p. Also shown is the contour for the Fourier integrals used in Section 5.

For non-trivial solutions to exist the determinant of the matrix $\mathbf{L}$ must be zero. In this case the equations for U and W are uncoupled leading to the dispersion equations $L_{UU} = 0$ and $L_{WW} = 0$. These relations could also be obtained by setting the denominator of the reflection and transmission coefficients to zero.

Setting Eq. (37b) to zero leads to the dispersion relation for the fluid loaded flexural waves and has been studied many times before (see, for example, Ref. [8]). The solutions for positive k consist of a subsonic, real solution together with complex solutions for the evanescent and leaky waves. Significant fluid loading is associated with $\bar{\omega} = O(\varepsilon^2)$, at which point all three terms in Eq. (37b) are significant. For completeness, we note that, for $\bar{\omega} > 1$, the subsonic wave is given by

$$k_s \sim k_0 \left(1 + \frac{(2\varepsilon)^2}{2\bar{\omega}(\bar{\omega}^2 - 1)^2} + O(\varepsilon^4) \right) \tag{38}$$

and the leaky wave by

$$k \sim k_b \left(1 + \frac{(2\varepsilon)\mathrm{i}}{4\bar{\omega}^{1/2}\sqrt{\bar{\omega} - 1}} + O(\varepsilon^2) \right). \tag{39}$$

When $\bar{\omega} < 1$ with $\bar{\omega} = O(1)$ (in the sense of Olver [21]), the subsonic wave is given by

$$k_s \sim k_b \left(1 + \frac{(2\varepsilon)}{4\bar{\omega}^{1/2}\sqrt{1 - \bar{\omega}}} + O(\varepsilon^2) \right). \tag{40}$$

None of these expressions are valid near $\bar{\omega} = 1$: for a discussion of their range of validity and distinguished scalings see Ref. [8].

For $\bar{\omega} = O(\varepsilon^2)$ an approximation can be obtained for the subsonic wave in the heavy fluid loading limit ($\bar{\omega} = \varepsilon^2 \Omega_0$ with $\Omega_0 \to 0$),

$$k \simeq k_b \left(\frac{2\varepsilon}{\bar{\omega}^{1/2}} \right)^{1/5}. \tag{41}$$

Approximations in other regions and matching relations around the coincidence frequency can be found in Refs. [8,9].

Setting Eq. (37a) to zero yields the dispersion relation for the symmetric (in-plane) plate wave. Re-writing in terms of the scaled wavenumber, $\zeta = k/k_p$, and the fluid loading parameter gives

$$(\zeta^2 - 1)\left(1 + \frac{2i\varepsilon\alpha_l\bar{\omega}}{\sqrt{1-(c_0/c_p)^2\zeta^2}}\right) - \frac{2i\varepsilon\alpha_p\bar{\omega}\zeta^2}{\sqrt{1-(c_0/c_p)^2\zeta^2}} = 0. \tag{42}$$

Treating α_l and α_p as $O(1)$ parameters (for the moment), this can be solved approximately by taking the fluid loading to be a perturbation ($\varepsilon \to 0$) [21]. One obtains

$$\zeta \sim 1 + \frac{(2\varepsilon)i\alpha_p\bar{\omega}}{2\sqrt{1-(c_0/c_p)^2}} + O(\varepsilon^2) \sim 1 + i\gamma^2\frac{2\rho_0 c_0}{\rho c_p}\frac{k_p h}{\sqrt{1-(c_0/c_p)^2}} + O(\varepsilon^2) \quad \text{as } \varepsilon \to 0 \tag{43}$$

the effect of fluid loading is thus to attenuate the symmetric wave by an amount depending on the ratio of the characteristic impedances of the plate to the fluid multiplied by $k_p h$.

When the usual inextendable plate theory is used, the case of an air-backed fluid loaded plate is identical to that of a fully immersed plate except that it has half the fluid loading (2ε is replaced by ε in expressions (38)–(41)). This is not the case, however, if the plate equations (20) and (21) are used. Setting $T_b = 0$ in the form for the acoustic field leads to a pair of coupled equations for the plate vibrations. Again, these can be written in the form of a matrix equation (36) but this time L_{UW} and L_{WU} are non-zero. The dispersion equation is found by setting the determinant of $\mathbf{L}$ equal to zero. Instead of separate dispersion relations for the symmetric and flexural waves, the combined dispersion relation

$$D(k,\beta) = (k^2 - k_p^2)(k^4 - k_b^4)\left(1 - \frac{i\mu}{\beta}\alpha_l\bar{\omega}^2\right) - \frac{i\mu}{\beta}k_b^4(k^2 - k_p^2) - \frac{i\mu}{\beta}\alpha_p\bar{\omega}^2k^2(k^4 - k_b^4) = 0 \tag{44}$$

is obtained.

The coupling between the two types of waves is small and there is no new structure in Eq. (44) as far as flexural waves are concerned. The approximate solutions (38)–(41) still hold for Eq. (44), the effects of coupling occurring at the next order in ε. Fig. 5 shows a comparison of the subsonic and leaky wave dispersion curves calculated using Eq. (37b) with those obtained from Eq. (44) for an air-backed steel plate in water. The fluid loading in Eq. (37b) has been halved, in the manner of the usual plate theory, for comparison purposes [1]. Branch (a) is the leaky wave, which tends towards k_b at high frequency (39). Branch (b) is purely real and is the subsonic wave. It tends towards $k_0 = \bar{\omega}^{1/2}k_b$ at high frequency (38), is close to k_b for frequencies below the coincidence frequency (40), and then increases steeply as the frequency tends towards zero in the heavy fluid loading region (41). The differences between dispersion curves calculated from the two different relations is typically less than 10^{-3} in this case.

The situation is more interesting when the symmetric modes are considered: writing Eq. (44) in terms of $\zeta = k/k_p$ and rearranging gives

$$(\zeta^2 - 1)\left[1 - \frac{i\varepsilon\alpha_l\bar{\omega}}{\sqrt{1-(c_0/c_p)^2\zeta^2}} + \frac{i\varepsilon}{\bar{\omega}(1-(c_0/c_p)^4\bar{\omega}^2\zeta^4)}\right] - \frac{i\varepsilon\alpha_p\bar{\omega}}{\sqrt{1-(c_0/c_p)^2\zeta^2}} = 0. \tag{45}$$

If $\bar{\omega} = O(1)$, the last two terms in the square brackets do not contribute until order ε^2 and the solution to first order is still given by Eq. (43) (with 2ε replaced by ε). If $\bar{\omega} = O(\varepsilon)$, however, the third term in the square brackets is $O(1)$ and will contribute at first order in ε. Setting $\bar{\omega} = \Omega_0\varepsilon$ gives

$$\zeta = \frac{k}{k_p} \sim 1 + \frac{\varepsilon^2\alpha_p\Omega_0^2}{2[\Omega_0^2(1-(c_0/c_p)^2)+1]} + \frac{i\varepsilon^2\alpha_p\Omega_0^3\sqrt{1-(c_0/c_p)^2}}{2[\Omega_0^2(1-(c_0/c_p)^2)+1]} + O(\varepsilon^4). \tag{46}$$

A comparison of the symmetric wave dispersion curve for a air-backed steel plate in water to that calculated using the uncoupled equation (37a) with half the fluid loading is shown in Fig. 6. The change in behaviour at

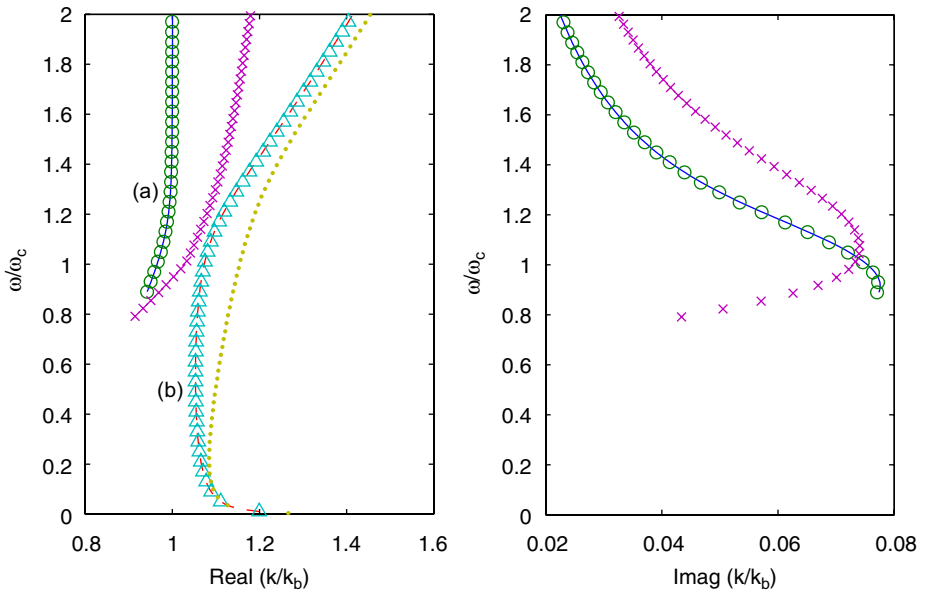

Fig. 5. Comparison of the dispersion curves obtained from the usual plate theory and those from the coupled relation (44) for an air-backed, water loaded, steel plate. Branch (a) is the leaky wave: the solid line is calculated from Eq. (37b) and the circles (◯) from Eq. (44). Branch (b) is the subsonic wave: the dashed line is from Eq. (37b) and the triangles (△) from Eq. (44). Also shown are the numerical dispersion curves for an air-backed, water loaded, steel plate calculated from the full elastic theory using the software Disperse: the crosses (×) are the leaky wave and the dots (•) the subsonic wave.

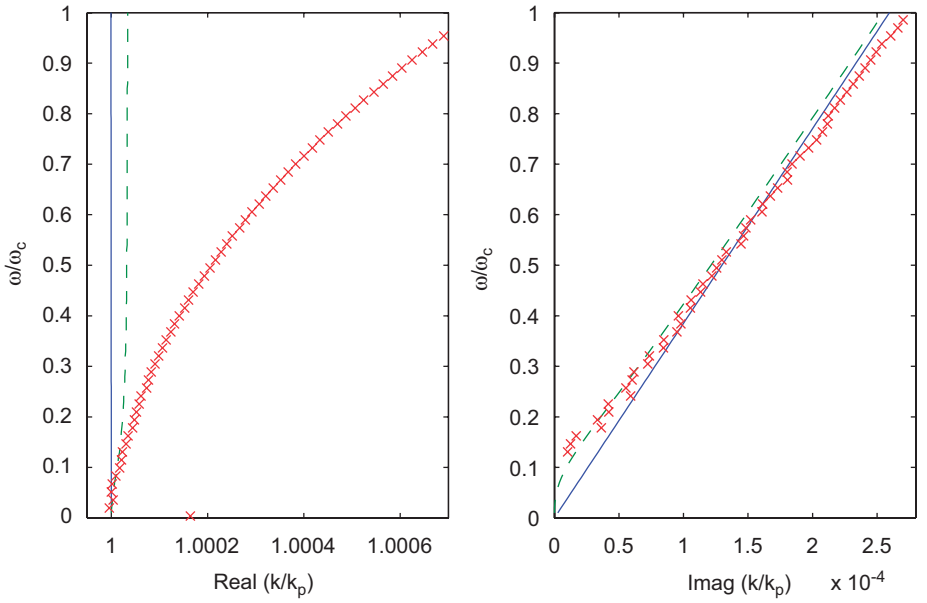

Fig. 6. Comparison of the dispersion curves obtained from the uncoupled dispersion equation (37a) (solid line) to that obtained from the coupled relation (44) (dashed line). The fluid loading parameter in the uncoupled case has been halved for comparison purposes. Also shown is the dispersion curve for the lowest order symmetric wave on an air-backed, water loaded, steel plate calculated from the full elastic equations using the software Disperse (×).

low frequency caused by the air-backing is most clearly seen in the imaginary part of the wavenumber. It should be noted that the usual plate theory [1] would give no attenuation for the symmetric wave, due to the absence of coupling to the fluid, and would have $k/k_p = 1$.

For completeness, Figs. 5 and 6 also include numerical solutions of the lowest order dispersion curves for an air-backed, water loaded, steel plate calculated from the full elastic theory using the software Disperse developed at Imperial College [22,23]. The differences between these curves and those calculated using thin plate theory, which are most notable for the flexural dispersion curves of Fig. 5, are primarily due to the neglect of transverse shear through the plate thickness: that thick plate theory must be used to obtain accurate predictions around the coincidence frequency is well known [1,3]. Nevertheless, thin plate theory predicts the qualitative physics extremely well and the two theories converge at low frequency. The numerical results for the symmetric wave in Fig. 6 seem to support the low-frequency behaviour predicted by the coupled relation (44), though the numerical solution becomes dominated by numerical error as the frequency tends to zero and starts to predict non-physical negative attenuations for the symmetric wave when $\bar{\omega} \lesssim 0.1$.

5. The line driven, fluid loaded, plate

Attention is now turned to the forced response of an air-backed, fluid loaded plate. The force is assumed to vary only in the x-direction and has the Fourier transform

$$f(x) = \frac{1}{2\pi}\int_{-\infty}^{\infty} F(k)\,\mathrm{e}^{\mathrm{i}kx}\,\mathrm{d}k. \tag{47}$$

The components of the displacement vector of the mid-plane of the plate are taken to be

$$u_x(x) = \frac{1}{2\pi}\int_{-\infty}^{\infty} U(k)\,\mathrm{e}^{\mathrm{i}kx}\,\mathrm{d}k, \tag{48}$$

$$w_0(x) = \frac{1}{2\pi}\int_{-\infty}^{\infty} W(k)\,\mathrm{e}^{\mathrm{i}kx}\,\mathrm{d}k \tag{49}$$

and using the wave equation in the fluid, the acoustic pressure in the half-space $z>h$ must have the form

$$p(x,z) = \frac{1}{2\pi}\int_{-\infty}^{\infty} P(k)\,\mathrm{e}^{\mathrm{i}kx+\mathrm{i}\beta(z-h)}\,\mathrm{d}k, \tag{50}$$

with β chosen as in Section 4. Substituting in the plate equations (20) and (21) and using Eq. (22) to guarantee continuity of the normal displacement at $z=h$, it is a straightforward matter to solve for P, W and U. They are given by

$$P = \frac{\mu F(k)}{\mathrm{i}\beta D(k,\beta)}[k_b^4(k^2-k_p^2) - \alpha_p\bar{\omega}^2k^2(k^4-k_b^4) - \alpha_l\bar{\omega}^2(k^4-k_b^4)(k^2-k_p^2)], \tag{51}$$

$$W = \frac{F(k)}{2h\rho c_b^2 D(k,\beta)}\left[(k^2-k_p^2)\left(1-\frac{2\mathrm{i}\mu}{\beta}\alpha_l\bar{\omega}^2\right) - \frac{2\mathrm{i}\mu}{\beta}\alpha_p\bar{\omega}^2k^2\right] \tag{52}$$

and

$$U = \frac{k\gamma F(k)}{2\mathrm{i}\rho c_p^2 D(k,\beta)}\left[(k^4-k_b^4) - \frac{2\mathrm{i}\mu}{\beta}k_b^4\right]. \tag{53}$$

The denominators, $D(k,\beta)$, are as given in Eq. (44).

The far-field acoustic pressure is obtained in the usual way from the saddle point contribution to the integral in Eq. (50) [1,8]. Taking $r=\sqrt{x^2+z^2}$ and θ to be the angle from the normal to the plate (z-axis), for sufficiently large k_0r the far-field pressure is given by

$$p(x,z) \sim \left(\frac{k_0}{2\pi r}\right)^{1/2} \mathrm{e}^{\mathrm{i}k_0r-\mathrm{i}\frac{\pi}{4}} P(k_0\sin\theta)\cos\theta. \tag{54}$$

For a discussion of the errors associated with this approximation see Ref. [5].

If $F(k)$ is assumed to be constant (a line driven plate), the angular intensity in the far field is given by

$$I(\theta) \propto |P(k_0 \sin\theta)|^2 \cos^2\theta. \tag{55}$$

A plot of the angular intensity, scaled by its value at $\theta = 0$, is given in Fig. 7, showing the peak in the far-field pressure near the coincidence angle for the symmetric wave, θ_p. There is also a (much wider) peak near the coincidence angle for the flexural wave, θ_b, when $\bar{\omega} > 1$. Since $|P(k_0 \sin\theta)| \to 1$ as both $\theta \to \theta_p$ and $\theta \to \theta_b$ the ratio of the peaks in the intensity at these points is given simply by $\cos^2\theta_p/\cos^2\theta_b$. The peak in the intensity near θ_p is very narrow however; by looking near θ_p for the points where $|P(k_0 \sin\theta)|^2$ is a fraction r of its peak value one can obtain an estimation of the angular width of this peak. Expanding in terms of ε and assuming α_l and α_p are small, one obtains (after much tedious algebra)

$$\Delta\theta \simeq \frac{\varepsilon\alpha_p\bar{\omega}}{\cos\theta_p}\frac{(1-r)^{1/2}}{r^{1/2}} + O(\varepsilon^2). \tag{56}$$

For steel in water $\Delta\theta = 0.084$ when $\bar{\omega} = 1.5$ if r is taken to be 0.25. Just before the peak in intensity there is a corresponding drop-out of similar width. One sees that, although the feature in the intensity near θ_p is broadband in terms of frequency, the angular width narrows with decreasing frequency making it less obvious at frequencies well below the coincidence frequency.

The far-field structural response of the plate can be calculated from the Fourier transforms (48) and (49). In both cases, the branch cut is chosen as in Fig. 4 and the contour of integration is then deformed around the branch. In doing this a contribution from the poles that have been crossed in deforming the contour is obtained giving

$$\text{Plate displacement} = 2\pi\mathrm{i} \times \sum(\text{Residues}) + \int(\text{Branch cut}). \tag{57}$$

In the far field of the plate, the integral around the branch cut can be approximated using Watson's Lemma [21]. In doing this, terms that decay faster than one over a fractional power of x are dropped, hence the only residue contribution that should be retained is that due to the subsonic (real) root [8].

One notes that, in general, the points $k = k_b$ and $k = k_p$ do not lie near the branch cut, hence the terms of order α_l and α_p can be dropped from the integrand. The branch cut contribution to the normal displacement is thus the same as that given by the inextendable theory, viz.,

$$w_0(x)_{\text{branch}} \simeq F_0\sqrt{\frac{k_0}{2\pi}}\frac{\mathrm{e}^{\mathrm{i}k_0 x - \mathrm{i}\frac{\pi}{4}}}{2h\rho c_b^2 \mu k_b^4}\frac{1}{x^{3/2}} + O(x^{-5/2}). \tag{58}$$

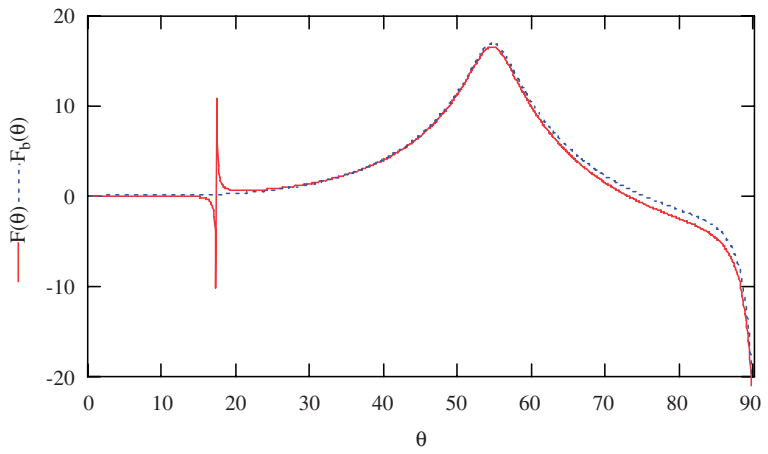

Fig. 7. Plot of the scaled far field intensity, $F(\theta) = 10\log_{10}|I(\theta)/I(0)|$, when $\bar{\omega} = 1.5$. This is compared with the result obtained from using only the bending wave contribution, $F_b(\theta)$, plotted as a dashed line.

To leading order in ε, the subsonic pole is the same as before hence the flexural wave contribution is as calculated previously [8].

The in-plane displacement, u_x, is calculated in a similar fashion. Again, because of the approximations involved in evaluating the branch-cut contribution, the only residue contribution that should be kept is that resulting from the subsonic pole. Since this is not expected to be near k_p, terms involving α_l and α_p can be dropped and

$$\underset{k\to k_s}{\text{Residue}}\, U(k) = \underset{k\to k_s}{\text{Residue}} \frac{k\gamma F_0}{2\mathrm{i}\rho c_p^2} \frac{\left[(k^4-k_b^4)-\dfrac{2\mathrm{i}\mu}{\beta}k_b^4\right]}{(k^2-k_p^2)\left[k^4-k_b^4-\dfrac{\mathrm{i}\mu}{\beta}k_b^4\right]}. \tag{59}$$

One see that the numerator of Eq. (59) is the dispersion relation for the flexural waves on a fully immersed fluid loaded plate; if the plate had fluid on both sides there would be no residue contribution from the subsonic pole but because of the free side the subsonic flexural wave couples to the in-plane displacements. The residue contribution then depends on the difference in the fluid loading and gives a contribution of the order of the fluid loading parameter, ε, when $\bar{\omega} = O(1)$.

The branch cut contribution to the normal displacement seems to be a structural acoustic wave caused by the acoustic near field of the force coupling back into the plate. Of course, the acoustic field can also couple into symmetric waves on the plate. Assuming k_p is not near k_0 so that terms involving α_p and α_l can be dropped, the branch cut contribution to the in-plane displacement is given by

$$u_x(x)_{\text{branch}} = \frac{\mathrm{i}\mathrm{e}^{\mathrm{i}k_0 x}}{2\pi}\int_0^\infty \hat{U}(k_0+\mathrm{i}s)\mathrm{e}^{-sx}\,\mathrm{d}s, \tag{60}$$

where

$$\hat{U}(k) = \frac{\gamma F_0 \mu\beta k k_b^4(k^4-k_b^4)}{\rho c_p^2(k^2-k_p^2)(\beta\mathrm{e}^2(k^4-k_b^4)^2+\mu^2 k_b^8)} \tag{61}$$

and β has been taken to have its value on the left-hand side of the branch cut. Eq. (60) is in a form suitable for application of Watson's Lemma [21] hence, for large x,

$$u_x(x)_{\text{branch}} \simeq \frac{\mathrm{i}\gamma \mathrm{e}^{\mathrm{i}k_0 x - \mathrm{i}\frac{\pi}{4}}}{\sqrt{2\pi}\rho c_p^2}\frac{k_0^{3/2}(k_0^4-k_b^4)F_0}{2\mu k_b^4(k_0^2-k_p^2)x^{3/2}} + O(x^{-5/2}). \tag{62}$$

When $\bar{\omega} = O(1)$, the subsonic residue contribution to the normal displacements of the mid-plane, $w_0(x)$, is $O(1)$ and dominates the flexural panel response. In the heavy fluid loading region, however, the residue contribution is $O(\varepsilon)$ [6] and the branch cut contribution (58) is significant. One might then wonder if the branch cut contribution (62) would also be significant?

The total energy in the panel at frequency ω is given by

$$E_{\text{total}} = 2h\int_{\text{mid plane}} \mathrm{d}S\left\{\frac{1}{2}\rho\omega^2(u_x u_x^* + w_0 w_0^*) + \frac{1}{2}\rho c_p^2 \frac{\mathrm{d}u_x}{\mathrm{d}x}\frac{\mathrm{d}u_x^*}{\mathrm{d}x} + \frac{1}{2}\rho c_b^2 \frac{\mathrm{d}^2 w_0}{\mathrm{d}x^2}\frac{\mathrm{d}^2 w_0^*}{\mathrm{d}x^2}\right\}. \tag{63}$$

The first two terms are the kinetic energy of the panel; equating the third term to the tensile energy in the plate and the fourth term to the flexural energy, one can examine the relative energy in these two contributions. Using Eqs. (58) and (62) one finds that if all the plate motion were in the branch-cut contributions the ratio of strain energy per unit area in the in-plane motion to that in the flexural wave is given approximately by

$$\frac{E_{\text{long}}}{E_{\text{flex}}} \simeq \gamma^2 h^2 \left(\frac{c_p}{c_b}\right)^2 \frac{\left(\dfrac{k_0^4}{k_b^4}-1\right)^2}{\left(\dfrac{k_0^2}{k_p^2}-1\right)^2} \quad \text{as } x\to\infty. \tag{64}$$

Since $c_b^2 = h^2 c_p^2/3$ this is an $O(1)$ quantity hence, if the structural acoustic contribution (58) for flexural waves is considered to be significant for the structural response, the structural acoustic symmetric wave may also need to be included.

In the heavy fluid loading limit, the residue contributions to the plate displacements can be calculated using the approximation (41) for the subsonic pole giving

$$w_0(x) \simeq \frac{-\pi \mathrm{i} \Omega_1^{3/10} F_0}{5h\rho c_b^2 k_b^3} \mathrm{e}^{\mathrm{i}k_s x} + \frac{F_0 k_0^{1/2}}{2\sqrt{2\pi}\mu h \rho c_b^2 k_b^4} \frac{\mathrm{e}^{\mathrm{i}k_0 x - \mathrm{i}\frac{\pi}{4}}}{x^{3/2}}, \tag{65}$$

$$u_x(x) \simeq \frac{-\pi\gamma}{5\rho c_p^2} \frac{\Omega_1^{1/10} k_b F_0}{(k_b^2 - \Omega_1^{1/5} k_p^2)} \mathrm{e}^{\mathrm{i}k_s x} + \frac{\mathrm{i}\gamma k_0^{3/2}(k^4 - k_b^4)}{2\sqrt{2\pi}\rho c_p^2 \mu k_b^4 (k^2 - k_p^2)} \frac{\mathrm{e}^{\mathrm{i}k_0 x - \mathrm{i}\frac{\pi}{4}}}{x^{3/2}}, \tag{66}$$

with $\bar{\omega} = \Omega_1 \varepsilon^2$, $k_s = k_b \Omega_1^{-1/10}$ and the approximations hold as $\Omega_1 \to 0$.

6. Thick shell theories

The thin shell theory gives a good qualitative picture of the physics of the fluid loaded plate however for accurate predictions above the coincidence frequency the effects of through thickness shear must be taken into account and a thick shell theory used [1]. Many of the thick shell theories used for structural vibration calculations, such as the Timoshenko–Mindlin plate theory, are based on an expansion of the form [18]

$$U_x(z) = u_0 - z\vartheta_1^u + z^2\vartheta_2^u + z^3\vartheta_3^u + \cdots, \tag{67a}$$

$$U_y(z) = v_0 - z\vartheta_2^v + z^2\vartheta_2^v + z^3\vartheta_3^v + \cdots, \tag{67b}$$

$$U_z(z) = w_0. \tag{67c}$$

As can be readily seen, expansions of this type still satisfy the Kirchoff–Love approximation and do not give any coupling between the acoustic fields and the in-plane vibrations. To regain the coupling to symmetric waves, the assumed form for U_z would have to be modified to include a term of at least order z.

7. Discussion

The preceding sections have shown how the effects of coupling between the in-plane plate vibrations and the acoustic field can be incorporated into thin plate theory. Although terms of the order of $\alpha_l \bar{\omega}^2 = k_l^2 h^2$ have been kept for consistency, these terms never give effects at leading order and can be dropped, simplifying the equations slightly. (In fact α_l has been used for book keeping—expansions are truncated at the point were α_l terms would contribute.) This amounts to dropping the first z dependant term in the continuity equation for the normal displacement (22). The second term leads to contributions of the form $\alpha_p \bar{\omega}^2/(k^2 - k_p^2)$. When $k^2 - k_p^2 = O(1)$ these contributions are of order $\gamma^2 k_p^2 h^2$ and would usually be dropped in thin shell theory. For $|k|$ near k_p, however, these terms become large and must be kept.

The coupling of the in-plane (symmetric wave) vibrations into the acoustic field is due to a tensile strain causing a small change in the thickness of the plate (and vice versa) through the Poisson's ratio of the material. Thus any shell theory (thick or thin) that takes inextendability of the normals to the mid-plane as one of its starting assumptions will not allow any coupling between the symmetric wave and the acoustic field for a flat plate. Although computing power has increased tremendously over the last few years, the complexity of many structural acoustic problems of practical interest means that a FE simulation is often performed using shell elements for the structure. Since many commercial FE codes were originally designed as structural codes, with the acoustic elements being added later, it is likely that in some codes the shell elements will be based on a shell theory that does not allow extension of the normals to the mid-plane. Of course on curved structures the normal displacements of the mid-plane are coupled to the in-plane displacements through curvature terms in the equation of motion, thus one would not expect to see any differences until the wavelength was much smaller than the radius of curvature. It is interesting to note that some differences between structural acoustic

calculations based on three-dimensional FE analysis and those based on shell elements have been observed [24], though the discrepancies have been conjectured to be caused by the contributions of non-propagating, higher order, Lamb waves to the boundary conditions at discontinuities.

The coupling between the in-plane vibrations of a plate and the acoustic field is generally small, nevertheless it can lead to significant effects in certain regimes—such as for a narrow range of angles in the case of the acoustic field or at very low frequencies in the case of the structural vibrations. These effects add to the richness of what appears, on the face of it, to be a simple physical system, that of a fluid loaded, forced, flat plate.

References

[1] M.C. Junger, D. Feit, *Sound, Structures and their Interaction*, The MIT Press, Cambridge, MA, 1986.
[2] F.J. Fahy, *Sound and Structural Vibration*, Academic Press, London, 1985.
[3] D. Feit, Pressure radiated by a point-excited elastic plate, *Journal of the Acoustical Society of America* 40 (6) (1966) 1489–1494.
[4] G. Maidanik, J.E.M. Kerwin, Influence of fluid loading on the radiation from infinite plates below the critical frequency, *Journal of the Acoustical Society of America* 40 (6) (1966) 1034–1038.
[5] D.G. Crighton, The free and forced waves on a fluid-loaded elastic plate, *Journal of Sound and Vibration* 63 (2) (1979) 225–235.
[6] D.G. Crighton, The green function of an infinite, fluid loaded membrane, *Journal of Sound and Vibration* 86 (3) (1983) 411–433.
[7] D.G. Crighton, Approximations to the admittances and free wavenumbers of fluid-loaded panels, *Journal of Sound and Vibration* 68 (1) (1980) 15–33.
[8] D.G. Crighton, The 1988 Rayleigh medal lecture: fluid loading—the interaction between sound and vibration, *Journal of Sound and Vibration* 133 (1) (1989) 1–27.
[9] C.J. Chapman, S.V. Sorokin, The forced vibration of an elastic plate under significant fluid loading, *Journal of Sound and Vibration* 281 (2005) 719–741.
[10] D. Feit, J.M. Cuschieri, Scattering of sound by a fluid-loaded plate with a distributed mass inhomogeneity, *Journal of the Acoustical Society of America* 99 (5) (1996) 2686–2700.
[11] A.W. Leissa, *Vibration of Plates*, NASA SP-160. Reprinted by the Acoustical & Society of America, 1993, 1969.
[12] A.J. Rudgers, P.S. Dubbelday, L.A. Fagerstrom, Extensional-wave and flexural-wave contributions to the sound field radiated by a fluid-loaded infinite plate, *Journal of the Acoustical Society of America* 80 (3) (1986) 932–950.
[13] W. Kohn, J.A. Krumhansl, E.H. Lee, Variational methods for dispersion relations and elastic properties of composite materials, *Transactions of the ASME Series E: Applied Mechanics* 94 (1972) 327–336.
[14] P.M. Morse, H. Feshbach, *Methods of Theoretical Physics*, McGraw-Hill Book Company, New York, 1953.
[15] C. Lanczos, *The Variational Principles of Mechanics*, University of Toronto Press, Canada, 1949.
[16] L.D. Landau, E.M. Lifshitz, *Theory of Elasticity*, third ed., Butterworth-Heinemann, Oxford, 1986.
[17] L.E. Kinsler, A.R. Frey, A.B. Coppens, J.V. Sanders, *Fundamentals of Acoustics*, fourth ed., Wiley, New York, 2000.
[18] K.M. Liew, C.W. Lim, S. Kitipornchai, Vibration of shallow shells: a review with bibliography, *Applied Mechanical Review* 50 (8) (1997) 431–444.
[19] L.M. Brekhovskikh, O.A. Godin, *Acoustics of Layered Media I*, second ed., Springer, Berlin, 1998.
[20] C.W. Chan, P. Cawley, Lamb waves in highly attenuative plastic plates, *Journal of the Acoustical Society of America* 104 (2) (1998) 874–881.
[21] F.W.J. Olver, *Asymptotics and Special Functions*, Academic Press. Reprinted by A K Peters, 1997, Natick, Massachusetts, 1974.
[22] M.J.S. Lowe, Matrix techniques for modelling ultrasonic waves in multilayered media, *IEEE Transactions on Ultrasonics Ferroelectrics and Frequency Control* 42 (1995) 525–542.
[23] B.N. Pavlakovic, M.J.S. Lowe, D.N. Alleyne, P. Cawley, Disperse: a general purpose program for creating dispersion curves, in: D.O. Thompson, D.E. Chimenti (Eds.), *Review of Progress in Quantitative NDE*, vol. 16, Plenum, New York, 1997, pp. 185–192.
[24] A. Tesei, M. Zampolli, J. Fawcett, D.S. Burnett, Verification of a 3-d structural-acoustic finite element tool against thin-shell scattering models, *Proceedings of the 7th European Conference on Underwater Acoustics*, Vol. 1, Delft, The Netherlands, 2004, pp. 431–436.